

# de Sitter Thick Brane Solution in Weyl Geometry

---

**Yu-Xiao Liu, Ke Yang\*, Yuan Zhong**

*Institute of Theoretical Physics, Lanzhou University, Lanzhou 730000, People's Republic of China*

*E-mail: liuyx@lzu.edu.cn, yangke09@lzu.cn, zhongy2009@lzu.cn*

**ABSTRACT:** In this paper, we consider a de Sitter thick brane model in a pure geometric Weyl integrable five-dimensional space-time, which is a generalization of Riemann geometry and is invariant under a so-called Weyl rescaling. We find a solution of this model via performing a conformal transformation to map the Weylian structure into a familiar Riemannian one with a conformal metric. The metric perturbations of the model are discussed. For gravitational perturbation, we get the effective modified Pöschl-Teller potential in corresponding Schrödinger equation for Kaluza-Klein (KK) modes of the graviton. There is only one bound state, which is a normalizable massless zero mode and represents a stable 4-dimensional graviton. Furthermore, there exists a mass gap between the massless mode and continuous KK modes. We also find that the model is stable under the scalar perturbation in the metric. The correction to the Newtonian potential on the brane is proportional to  $e^{-3r\beta/2}/r^2$ , where  $\beta$  is the de Sitter parameter of the brane. This is very different from the correction caused by a volcano-like effective potential.

**KEYWORDS:** Extra Dimensions, Brane world, de Sitter Thick Branes, Weyl Geometry.

---

\*Corresponding author.

---

## Contents

<b>1. Introduction</b>	<b>1</b>
<b>2. Weyl geometry</b>	<b>3</b>
<b>3. The model</b>	<b>4</b>
<b>4. Metric perturbations</b>	<b>10</b>
<b>5. The Effective Newtonian Potential</b>	<b>15</b>
<b>6. Conclusion</b>	<b>20</b>
<b>7. Acknowledgments</b>	<b>20</b>

---

## 1. Introduction

The possibility that our world is trapped in a four-dimensional submanifold (called brane) embedded in a fundamental multi-dimensional space-time (called bulk) has been increasing interest during recent years (see [1, 2] for summary of introduction, and reference therein). The strong motivations originate from the string/M theory. With the help of the brane scenario, one could possibly solve some disturbing problem of high-energy physics, such as the hierarchy problems (the problem of why the electroweak scale  $M_{EW} \sim 1$  TeV is so different from the Planck scale  $M_{pl} \sim 10^{16}$  TeV ) and the cosmological constant problem [3, 4, 5, 6, 7, 8]. In this scenario, Standard Model matter fields are confined to a 3-brane, while the gravity could propagate in the whole bulk. The most well-known models within are Arkani-Hamed-Dimopoulos-Dvali (ADD) [3, 4] and Randall-Sundrum (RS) [5, 6] models put forward in the end of 90's. They can achieve a Newtonian gravitation law in macroscopic scale, which is compatible with the observational fact. What preeminence in RS model is that it suggests a possibility that the extra dimensions may not be compact any more, namely the size of extra dimensions can be even infinite.

However, both the models above are assumed that the brane is infinitely thin. Although with the idealized models many interesting results have been obtained, from a more realistic point of view, a brane should have the thickness. For this reason, the emphasis of study has shifted toward the thick brane scenario [9, 10, 11, 12, 13, 14, 15, 16, 17, 18, 19, 20, 21, 22, 23, 24, 25, 26, 27, 28, 29, 30, 31, 32, 33]. An interesting feature of thick brane scenario based on gravity coupled to scalar is that one can achieve a brane naturally without introducing a delta function by hand in the action to create a brane. And the scalar could further provide the “material” to make the thick brane. In many multidimensional field theories

coupled to gravity there are solutions of topological defects. They have lead to a richer variety of thick brane worlds [16].

Most investigations of brane worlds are considered in Riemann geometry. In this paper, we are interested in the thick branes based on a Weyl-integrable geometry, which is a generalization of Riemann geometry.

$$\text{Metric-affine} \xrightarrow{Q-\text{tr}(Q)=0} \text{Weyl-Cartan} \begin{cases} \xrightarrow{T \neq 0, Q=0} \text{Riemann-Cartan} \\ \xrightarrow{T=0, Q \neq 0} \text{Weyl} \\ \xrightarrow{T=0, Q=0} \text{Riemann} \end{cases} \quad (1.1)$$

As is shown in (1.1) [34], we can see there are two type generalizations of Riemann geometry, namely, the Riemann-Cartan and the Weyl geometry. In Riemann-Cartan geometry, the connection is asymmetric and the antisymmetric piece of the connection is represented as torsion  $T$  introduced by Cartan. In contrast to Riemann-Cartan geometry, the connection is no longer metric compatible in Weyl geometry, i.e., it involves a geometric scalar  $\omega$  in the definition of connection and the covariant derivative of metric tensor is non-vanishing. The field related to this violation of the metricity condition is called nonmetricity  $Q$ . So Weyl geometry allows for possible variations in the length of vectors during parallel transport. When  $T = 0$  the Riemann-Cartan geometry degenerates into Riemann, and when  $Q = 0$  the Weyl geometry also degenerates into Riemann geometry. More precisely, a Weyl geometry is an affine manifold specified by  $(g_{MN}, \omega)$ , where  $g_{MN}$  is the metric tensor and  $\omega$  is the geometric scalar  $\omega$ . Since a conformal transformation can map a Weyl manifold into a Riemann one, the particular type of gauge geometries is called conformally Weyl or Riemann integrable space-time [35]. On the other hand, Weyl integrable manifold is invariant under a Weyl rescaling (see, (2.2) for detail), when this invariance is broken, the Weyl scalar function  $\omega$  transforms into an observable field which generates the smooth thick brane configurations. Thus in Weyl geometry the fundamental role in the generation of thick brane configurations is ascribed to the geometric Weyl scalar field, which is not a bulk field now.

In Refs. [14, 35, 36, 37], the authors have studied brane world scenario in the frame of Weyl geometry, and achieved various solutions respected to Minkowski thick branes. For most of these branes [35, 36], there exist a single bound state which represents a stable 4-dimensional graviton and the continuum spectrum of massive modes of KK excitations without mass gap for a volcano potential. While in [14], the KK spectrum is quantized for an infinite square-like potential wall, and in [37], there exist one massless bound state, one massive KK bound state and the delocalized continuum spectrum for a modified Pöschl-Teller potential. These give a claim that Weylian structures mimic, classically, quantum behavior does not constitute a generic feature of these geometric manifolds [36]. In Refs. [38, 39], the authors have considered the localization and mass spectrum problems of matter fields on these various Minkowski thick branes. An interesting study in [39] shows that for scalars there are two bound states (one is normalizable massless mode), for spin one vectors there is only one normalizable massless bound state, and for spin half fermions, the total number of bound states is determined by the coupling constant  $\eta$ : when  $\eta = 0$ , there

are no any localized fermion KK modes including zero modes for both left and right chiral fermions, and when  $\eta > 0$  ( $\eta < 0$ ), the number of bound states of right chiral fermions is one less (more) than that of left chiral fermions and in both cases ( $\eta > 0$  and  $\eta < 0$ ), only one of the zero modes for left chiral fermions and right chiral fermions is bound and normalizable.

We will consider a de Sitter thick brane based on gravity coupled to scalars on a Weyl integrable manifold in this paper, and try to find a solution of de Sitter thick brane from a pure geometrical Weyl action in five dimensions. The organization of the paper is as follows: In Sec. 2, we briefly review the Weyl geometry. In Sec. 3, we consider a de Sitter thick brane solution on the weyl manifold and find a solution of the model. In Sec. 4, we briefly consider the gravitational and scalar perturbations of the structure. In Sec. 5, we derive the effective Newtonian potential on the brane. And finally, the conclusion is given in Sec. 6.

## 2. Weyl geometry

A non-Riemann generalization of Kaluza-Klein theory is based on the following five-dimensional action [14]:

$$S_5^W = \int_{M_5^W} \frac{d^5x \sqrt{|g|}}{16\pi G_5} e^{-\frac{3}{2}\omega} \left[ R - 3\xi (\nabla\omega)^2 - 6U(\omega) \right], \quad (2.1)$$

where  $M_5^W$  is a five-dimensional Weyl-integrable manifold specified by the pair  $(g_{MN}, \omega)$ ,  $g_{MN}$  is the metric ( $M, N = 0, 1, 2, 3, 5$ ) and  $\omega$  is a scalar function. In this manifold the Weylian Ricci tensor reads  $R_{MN} = \Gamma_{MN,A}^A - \Gamma_{AM,N}^A + \Gamma_{MN}^P \Gamma_{PQ}^Q - \Gamma_{MQ}^P \Gamma_{NP}^Q$ , where the affine connection of  $M_5^W$  is  $\Gamma_{MN}^P = \{_{MN}^P\} - \frac{1}{2}(\omega_{,M} \delta_N^P + \omega_{,N} \delta_M^P - g_{MN} \omega^{,P})$  with  $\{_{MN}^P\}$  the Christoffel symbol. The parameter  $\xi$  is a coupling constant, and  $U(\omega)$  is a self-interaction potential for the scalar field. Since the scalar field  $\omega$  enters in the definition of the affine connection of the Weyl manifold, the Weyl action is actually pure geometrical.

Weyl integrable manifold is invariant under the Weyl rescaling,

$$g_{MN} \rightarrow \Omega^2 g_{MN}, \quad \omega \rightarrow \omega + \ln \Omega^2, \quad \xi \rightarrow \xi / (1 + \partial_\omega \ln \Omega^2)^2, \quad (2.2)$$

where  $\Omega^2$  is a smooth function on  $M_5^W$ . In general, this invariance is broken by the self-interaction potential  $U(\omega)$ . But from the relation (2.2), we know that  $U \rightarrow \Omega^{-2}U$  is the only transformation preserves such an invariance. Thus the potential will be  $U(\omega) = \lambda e^{-\omega}$ , where  $\lambda$  is a coupling constant. When the Weyl invariance is broken, the scalar field could transform from a geometric object into an observable degree of freedom which generates the smooth thick brane configurations.

In order to find solutions of the above theory, we shall use the conformal technique to map the Weyl frame into the Riemann one. Under the conformal transformation  $g_{MN} = e^\omega \hat{g}_{MN}$ , the Weylian affine connection becomes the Christoffel symbol  $\Gamma_{MN}^P \rightarrow \{_{MN}^P\}$ , and the Weylian Ricci tensor becomes the Riemannian Ricci tensor. In consequence, via the conformal transformation, one recovers the Riemannian structure on the manifold  $M_5^R$ .

Now the Weylian action (2.1) is mapped into a Riemann one:

$$S_5^R = \int_{M_5^R} \frac{d^5x \sqrt{|\hat{g}|}}{16\pi G_5} \left[ \hat{R} - 3\xi(\hat{\nabla}\omega)^2 - 6\hat{U}(\omega) \right], \quad (2.3)$$

where  $\hat{U}(\omega) = e^\omega U(\omega)$  and all the hatted magnitudes and operators refer to the Riemann frame. Thus, one obtains a theory which describes five-dimensional gravity coupled to a scalar field with a self-interaction potential in the Riemann frame.

By considering the variation of the metric  $\hat{g}^{MN}$  and the scalar function  $\omega$ , we have the set of field equations from (2.3):

$$\hat{G}_{MN} = -\frac{3}{2}\xi\hat{g}_{MN}(\hat{\nabla}\omega)^2 + 3\xi\hat{\nabla}_M\omega\hat{\nabla}_N\omega - 3\hat{g}_{MN}\hat{U}(\omega), \quad (2.4a)$$

$$\hat{\square}\omega = \frac{1}{\xi} \frac{d\hat{U}(\omega)}{d\omega}. \quad (2.4b)$$

### 3. The model

In Refs. [14, 35, 36, 37], the authors studied thick brane solutions to the theory (2.1), and they considered the metric that respects four-dimensional Poincaré invariance:

$$ds_5^2 = e^{2A(y)} \eta_{\mu\nu} dx^\mu dx^\nu + dy^2, \quad (3.1)$$

i.e., the Minkowski thick brane solutions in Weyl Geometry, where  $e^{2A(y)}$  is the warp factor and  $y$  stands for the extra coordinate. The localization and mass spectrum problems of matter fields on the Minkowski thick branes were discussed in Refs. [38, 39].

The authors of [14] have considered the problem of  $Z_2$ -symmetric manifolds. They have chosen  $\xi = -(1+k)/(4k)$  and left  $k$  as an arbitrary parameter except for  $k = -4/3$ . The following solution was found:

$$\omega(y) = \frac{2k}{4-3k} \ln \left[ \cosh \left( \sqrt{\frac{4-3k}{1-k}} 2\lambda y \right) \right], \quad (3.2a)$$

$$e^{2A(y)} = \left[ \cosh \left( \sqrt{\frac{4-3k}{1-k}} 2\lambda y \right) \right]^{\frac{2}{4-3k}}. \quad (3.2b)$$

The authors of [35] have considered another simplified case when  $k = -4/3$  and left  $\xi$  as an arbitrary parameter except for  $\xi = -1/16$ . Their solution is

$$\omega(y) = -\frac{2}{1+16\xi} \ln \left\{ \frac{\sqrt{-8\lambda(1+16\xi)}}{c_1} \cosh [c_1 (y - c_2)] \right\}, \quad (3.3a)$$

$$e^{2A(y)} = \left\{ \frac{\sqrt{-8\lambda(1+16\xi)}}{c_1} \cosh [c_1 (y - c_2)] \right\}^{\frac{3}{2(1+16\xi)}}. \quad (3.3b)$$

Obviously, the first solution (3.2) is symmetric with respect to  $y$  coordinate, and the second solution is also a symmetric one if we perform a translation of  $y$  axis.

In this paper, we consider a de Sitter thick brane solution in a pure geometric five-dimensional Weyl space-time. The line element for the space-time with planar-parallel symmetry is assumed as

$$\begin{aligned} ds_5^2 &= g_{MN} dx^M dx^N \\ &= e^{2A(y)} q_{\mu\nu} dx^\mu dx^\nu + dy^2 \\ &= e^{2A(y)} \left( -dt^2 + e^{2\beta t} dx^i dx^i \right) + dy^2, \end{aligned} \quad (3.4)$$

where  $\beta$  is the de Sitter parameter and related to the 4-dimensional cosmological constant of the brane. Under the conformal transformation  $g_{MN} = e^\omega \hat{g}_{MN}$ , the de Sitter metric (3.4) is mapped into

$$\begin{aligned} d\hat{s}_5^2 &= \hat{g}_{MN} dx^M dx^N \\ &= e^{2\sigma(y)} \left( -dt^2 + e^{2\beta t} dx^i dx^i \right) + e^{-\omega(y)} dy^2, \end{aligned} \quad (3.5)$$

where  $2\sigma = 2A - \omega$ .

Now the expressions for Ricci tensor and the scalar curvature in the Riemann frame read

$$\begin{aligned} \hat{R}_{00} &= (\sigma'' + 4\sigma'^2 + \frac{1}{2}\sigma'\omega') e^{2A} - 3\beta^2, \\ \hat{R}_{ij} &= -(\sigma'' + 4\sigma'^2 + \frac{1}{2}\sigma'\omega') e^{2(A+\beta t)} \eta_{ij} + 3\beta^2 e^{2\beta t} \eta_{ij}, \\ \hat{R}_{55} &= -4(\sigma'' + \sigma'^2 + \frac{1}{2}\sigma'\omega'), \\ \hat{R} &= -4(2\sigma'' + 5\sigma'^2 + \sigma'\omega') e^\omega + 12\beta^2 e^{-2\sigma}, \end{aligned} \quad (3.6)$$

where the prime denotes derivative with respect to the fifth coordinate  $y$ . The five-dimensional stress-energy tensor is given by

$$\hat{T}_{MN} = \hat{R}_{MN} - \frac{1}{2} \hat{g}_{MN} \hat{R}, \quad (3.7)$$

thus, its four-dimensional and five-dimensional components are given through the following expressions:

$$\begin{aligned} \hat{T}_{00} &= -3 \left( \sigma'' + 2\sigma'^2 + \frac{1}{2}\sigma'\omega' \right) e^{2A} + 3\beta^2, \\ \hat{T}_{ij} &= 3 \left( \sigma'' + 2\sigma'^2 + \frac{1}{2}\sigma'\omega' \right) e^{2(A+\beta t)} \eta_{ij} - 3\beta^2 e^{2\beta t} \eta_{ij}, \\ \hat{T}_{55} &= 6\sigma'^2 - 6\beta^2 e^{-2A}. \end{aligned} \quad (3.8)$$

For simplicity, using the pair of variables  $X \equiv \omega'$  and  $Y \equiv 2A'$ , we obtain a set of equations from (2.4), (3.5) and (3.6):

$$X' + 2XY - \frac{3}{2}X^2 = \frac{1}{\xi} \frac{d\hat{U}(\omega)}{d\omega} e^{-\omega}, \quad (3.9a)$$

$$Y' + 2Y^2 - \frac{3}{2}XY = \left( \frac{1}{\xi} \frac{d\hat{U}}{d\omega} - 4\hat{U} \right) e^{-\omega} + 6\beta^2 e^{-2A}, \quad (3.9b)$$

$$Y^2 - 2XY + (1 - \xi) X^2 = -2e^{-\omega} \hat{U}(\omega) + 4\beta^2 e^{-2A}. \quad (3.9c)$$

Though we have got the field equations by performing a conformal transformation  $\hat{g}_{AB} = e^{-\omega} g_{AB}$  to map the Weyl manifold structure into the Riemann one, the solutions corresponding to the Eqs. (3.9) are harder to get than the similar equations in Ref. [14] for the flat brane (just set  $\beta = 0$  in Eqs. (3.9)). So, in order to simplify the model, we make a coordinate transformation of the form  $dy = e^{A(z)} dz$ . Then the metric (3.5) will be rewrote as:

$$d\hat{s}_5^2 = e^{2\sigma(z)} (q_{\mu\nu} dx^\mu dx^\nu + dz^2) = e^{2\sigma(z)} \left( -dt^2 + e^{2\beta t} dx^i dx^i + dz^2 \right). \quad (3.10)$$

Now repeating our calculation above, the expressions for the Ricci tensor and the scalar curvature corresponding to the metric (3.10) in the Riemann frame read:

$$\begin{aligned} \hat{R}_{00} &= \sigma'' + 3\sigma'^2 - 3\beta^2, \\ \hat{R}_{ij} &= -(\sigma'' + 3\sigma'^2 - 3\beta^2) e^{2\beta t} \eta_{ij}, \\ \hat{R}_{55} &= -4\sigma'', \\ \hat{R} &= -(8\sigma'' + 12\sigma'^2 - 12\beta^2) e^{-2\sigma}. \end{aligned} \quad (3.11)$$

The stress-energy tensor is given through the following expressions:

$$\begin{aligned} \hat{T}_{00} &= -3(\sigma'' + \sigma'^2 - \beta^2), \\ \hat{T}_{ij} &= 3(\sigma'' + \sigma'^2 - \beta^2) e^{2\beta t} \eta_{ij}, \\ \hat{T}_{55} &= 6(\sigma'^2 - \beta^2). \end{aligned} \quad (3.12)$$

So the set of field equations with the new conformally metric (3.10) now read

$$\xi \omega'^2 = \sigma'^2 - \sigma'' - \beta^2, \quad (3.13a)$$

$$\hat{U}(\omega) = \frac{1}{2} e^{-2\sigma} (-3\sigma'^2 - \sigma'' + 3\beta^2), \quad (3.13b)$$

$$\frac{1}{\xi} \frac{d\hat{U}(\omega)}{d\omega} = e^{-2\sigma} (3\sigma' \omega' + \omega''), \quad (3.13c)$$

where the prime denotes derivative with respect to  $z$ . If we choose the parameter  $\xi = 1/3$ , and define  $\hat{V}(\omega) = 3\hat{U}(\omega)$ , we can rewrite Eq. (3.13) as follows:

$$\omega'^2 = 3(\sigma'^2 - \sigma'' - \beta^2), \quad (3.14a)$$

$$\hat{V}(\omega) = \frac{3}{2} e^{-2\sigma} (-3\sigma'^2 - \sigma'' + 3\beta^2), \quad (3.14b)$$

$$\frac{d\hat{V}(\omega)}{d\omega} = e^{-2\sigma} (3\sigma' \omega' + \omega''). \quad (3.14c)$$

This set of equations is identical with the field equations of the de Sitter thick brane in the Riemann geometry [13, 40, 41, 42, 43, 44, 45, 46]. Here, we can achieve a  $Z_2$ -symmetric solution refer to  $z$  coordinate when we consider a symmetric domain wall de Sitter expansion in five dimensions for a sine-Gordon potential [47, 48]

$$\hat{V}(\omega) = 3\hat{U}(\omega) = p \cos^2(q\omega) + v \quad (3.15)$$

with  $p = 15\beta^2$ ,  $q = 1/\sqrt{3}$ ,  $v = -15\beta^2/2$  and  $\beta > 0$ . The warp factor of the metric (3.10) on Riemann manifold and the scalar  $\omega$  are

$$e^{2\sigma(z)} = \operatorname{sech}(2\beta z), \quad (3.16a)$$

$$\omega(z) = \frac{\sqrt{3}}{2} \arctan[\sinh(2\beta z)]. \quad (3.16b)$$

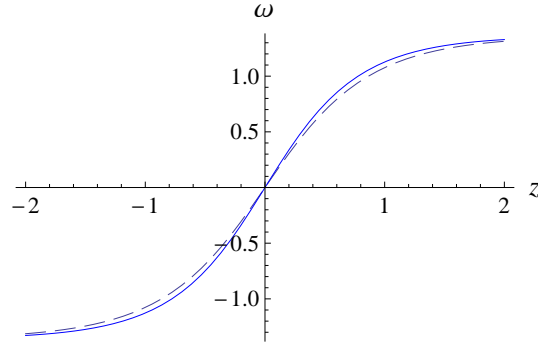


**Figure 1:** The shapes of the scalar  $\omega$  in  $z$  coordinate. The parameter  $\beta$  is set to  $\beta = 0.9$  for the dashed line, and  $\beta = 1$  for the thin line.

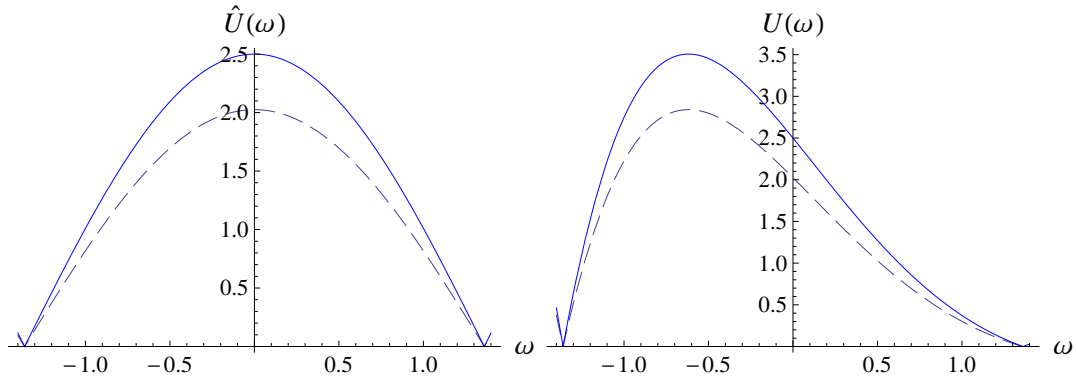


**Figure 2:** The shapes of the potential  $\hat{U}(\omega)$  on the Riemann manifold (left) and the potential  $U(\omega)$  on the Weyl manifold (right). The parameter  $\beta$  is set to  $\beta = 0.9$  for the dashed line, and  $\beta = 1$  for the thin line.

From  $\hat{U}(\omega) = e^\omega U(\omega)$  and Eq. (3.15), we have the potential in the original action (2.1) on the Weyl manifold:

$$U(\omega) = 5\beta^2 \left[ \cos^2\left(\frac{\omega}{\sqrt{3}}\right) - \frac{1}{2} \right] e^{-\omega}. \quad (3.17)$$

From the relation  $e^{2\sigma} = e^{2(A-\omega)}$ , the warp factor  $e^{2A(z)}$  is given by

$$e^{2A(z)} = e^{\sqrt{3} \arctan[\sinh(2\beta z)]} \operatorname{sech}(2\beta z). \quad (3.18)$$

The shapes of the scalar  $\omega$ , the potentials  $\hat{U}(\omega)$  in the Riemannian structure and  $U(\omega)$  in the Weylian one, the warp factors  $e^{2\sigma}$  on the Riemann manifold and  $e^{2A}$  on the Weyl



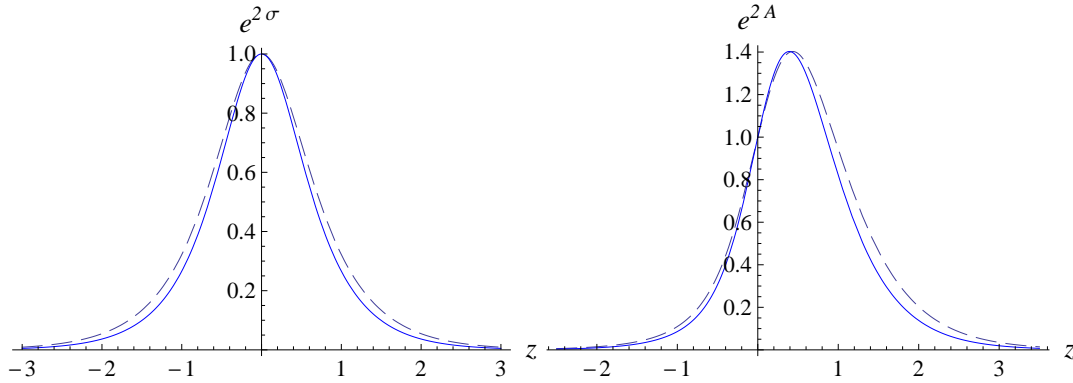


**Figure 3:** The shapes of the warp factor  $e^{2\sigma}$  on Riemann manifold (left) and the warp factor  $e^{2A}$  on Weyl manifold (right). The parameter  $\beta$  is set to  $\beta = 0.9$  for the dashed line, and  $\beta = 1$  for the thin line.

manifold are shown in Figs. 1, 2 and 3, respectively. We can see that the scalar field takes values  $\pm\sqrt{3}\pi/4$  at  $z \rightarrow \pm\infty$ , corresponding to the two minima of the potential with cosmological constant  $\Lambda = 0$ . So the scalar is actually a kink solution, which provides a thick brane realization of the brane world as a domain wall in the bulk. In the Riemannian structure, the potential  $\hat{U}(\omega)$  and the warp factor are symmetric, but in the Weylian one, they are asymmetric.

Now from  $dy = e^{A(z)}dz$ , we can calculate the relation between the original space-time coordinate  $y$  in metric (3.5) and  $z$  in (3.10). However, we could only achieve a numerical function curve  $y = y(z)$  in Fig. 4 (left). The scalar field in  $y$  coordinate is plotted in Fig. 4 (right).

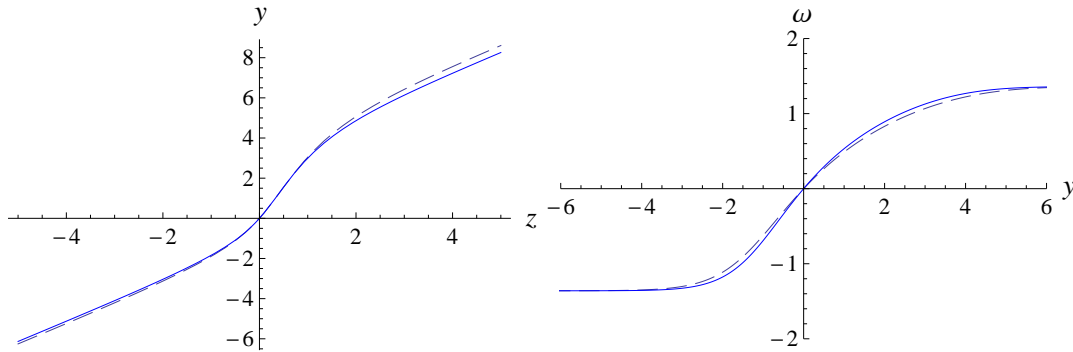


**Figure 4:** The relation of the coordinates  $y$  and  $z$  (left) and the scalar field  $\omega$  in  $y$  coordinate (right). The parameter  $\beta$  is set to  $\beta = 0.9$  for the dashed line, and  $\beta = 1$  for the thin line.

We can find that the scalar  $\omega(y)$  is asymmetric but still a kink-like solution in  $y$  coordinate. We display the shapes of the warp factors  $e^{2\sigma(y)}$  and  $e^{2A(y)}$  in Fig. 5. The figure shows that the warp factor  $e^{2\sigma(y)}$  is no longer symmetric even in the Riemannian structure, though the maximum is still at the origin of the  $y$  coordinate. So it will not

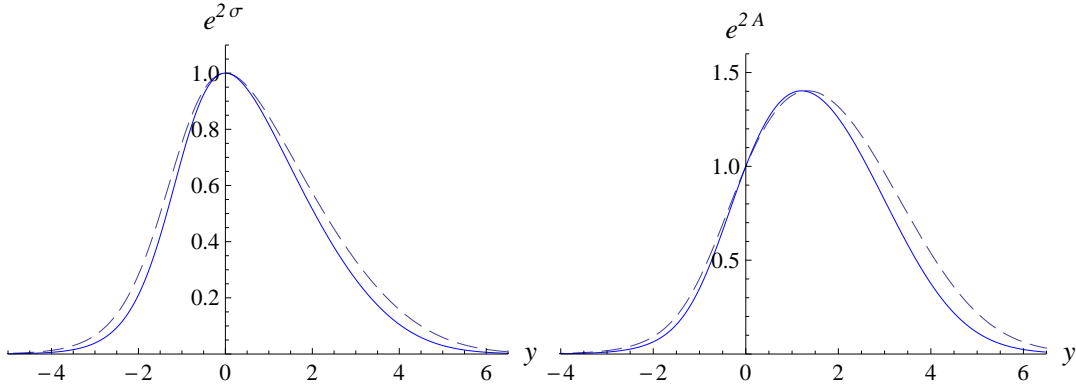


**Figure 5:** The shapes of the warp factors  $e^{2\sigma(y)}$  on the Riemann manifold (left) and  $e^{2A(y)}$  on the Weyl manifold (right). The parameter  $\beta$  is set to  $\beta = 0.9$  for the dashed line, and  $\beta = 1$  for the thin line.

preserve  $Z_2$ -symmetry in the Riemann manifold in the  $y$  coordinate.

The energy density of the scalar matter on the Riemann manifold is given by the null-null component of the stress-energy tensor (3.12):

$$\begin{aligned}\hat{\rho}(z) &= \hat{T}_{00} = -3(\sigma'' + \sigma'^2 - \beta^2) \\ &= 9\beta^2 \operatorname{sech}^2(2\beta z).\end{aligned}\tag{3.19}$$

The shape of the energy density  $\hat{\rho}$  is plotted in Fig. 6 in  $z$  and  $y$  coordinates, respectively. The figures clearly show that the energy density  $\hat{\rho}$  distributes along extra coordinate, so it does not stand for a thin brane any more, and  $1/\beta$  plays the role of the brane thickness. The energy density has a maximum at the origin of the coordinate, and vanishes asymptotically at  $y = \pm\infty$ , so the scalar matter mainly distributes on the brane. The energy density is symmetric in  $z$  coordinate while asymmetric in  $y$ .

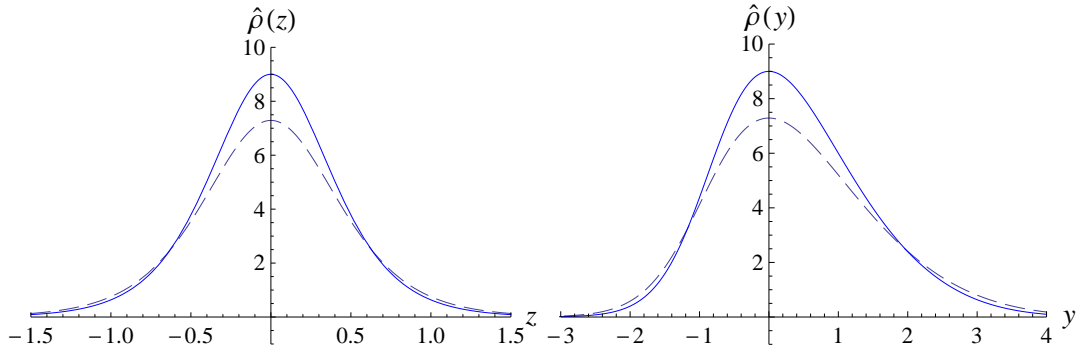


**Figure 6:** The shapes of the energy density  $\hat{\rho}$  in  $z$  coordinate (left) and in  $y$  coordinate (right) on the Riemann manifold. The parameter  $\beta$  is set to  $\beta = 0.9$  for the dashed line, and  $\beta = 1$  for the thin line.

#### 4. Metric perturbations

Firstly, we consider the gravitational perturbation in the metric (3.10):

$$\begin{aligned} d\hat{s}_5^2 &= e^{2\sigma(z)} [(q_{\mu\nu} + h_{\mu\nu}(x, z)) dx^\mu dx^\nu + dz^2] \\ &= e^{2\sigma(z)} [-dt^2 + e^{2\beta t} dx^i dx^i + h_{\mu\nu}(x, z) dx^\mu dx^\nu + dz^2]. \end{aligned} \quad (4.1)$$

Here  $h_{\mu\nu}$  is the tensor perturbation of the metric, and it satisfies the transverse traceless condition [9, 13, 49],

$$h_\mu{}^\mu = \nabla^\nu h_{\mu\nu} = 0, \quad (4.2)$$

where  $\nabla$  denotes the covariant derivative with respect to the four-dimensional metric  $q_{\mu\nu}$ . The equation for  $h_{\mu\nu}$  is given by [13, 49]

$$h''_{\mu\nu} + 3\sigma' h'_{\mu\nu} + \square h_{\mu\nu} - 2\beta^2 h_{\mu\nu} = 0, \quad (4.3)$$

where  $\square \equiv q^{\mu\nu} \nabla_\mu \nabla_\nu$ . Here we can define the four-dimensional mass of a KK excitation as

$$\square h_{\mu\nu} - 2\beta^2 h_{\mu\nu} = m^2 h_{\mu\nu}. \quad (4.4)$$

Furthermore, we can decompose  $h_{\mu\nu}$  in the form

$$h_{\mu\nu}(x, z) = e^{-3\sigma/2} \varepsilon_{\mu\nu}(x) \Psi(z), \quad (4.5)$$

where  $\varepsilon_{\mu\nu}$  satisfies the transverse traceless condition

$$\varepsilon_\mu{}^\mu = \nabla^\nu \varepsilon_{\mu\nu} = 0. \quad (4.6)$$

Now considering (4.4) and (4.5), Eq. (4.3) can be rewritten as

$$-\Psi''(z) + \left( \frac{3}{2} \sigma'' + \frac{9}{4} \sigma'^2 \right) \Psi(z) = m^2 \Psi(z). \quad (4.7)$$

So it turns into a Schrödinger equation form, and the effective potential reads

$$V_g(z) = \frac{3}{2} \sigma'' + \frac{9}{4} \sigma'^2 = \frac{3}{4} \beta^2 [3 - 7 \operatorname{sech}^2(2\beta z)]. \quad (4.8)$$

The spectrum of the eigenvalue  $m^2$  parameterizes the spectrum of the observed four-dimensional graviton masses. And obviously, there exists a zero mode which refers to  $m = 0$ . From Eq. (4.7) with  $m = 0$ , we can easily get

$$\Psi_0(z) = c_0 e^{3\sigma(z)/2} = c_0 \operatorname{sech}^{3/4}(2\beta z). \quad (4.9)$$

It can easily be seen that this zero mode is normalizable, and  $c_0 = \sqrt{\frac{2\beta\Gamma(5/4)}{\sqrt{\pi}\Gamma(3/4)}}$  is a normalization constant. So the 4D gravity can be produced by the zero mode [6, 9, 10, 11, 13].

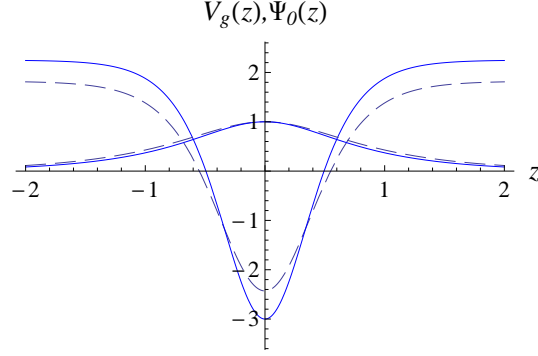


**Figure 7:** The shapes of the potential  $V_g(z)$  (concave) and the KK zero mode  $\Psi_0(z)$  (convex). The parameter  $\beta$  is set to  $\beta = 0.9$  for the dashed line, and  $\beta = 1$  for the thin line.

The shapes of the potential and the zero mode are plotted in Fig. 7. The figure shows that the gravitational zero mode localizes around  $z = 0$ , and vanishes at each side asymptotically. The effective potential is actually a modified Pöschl-Teller potential. From (4.8) we know that the potential barriers at each side approach to a maximum  $V_g^{max} = 9\beta^2/4$  when  $z \rightarrow \pm\infty$ , so there will exist a set of continuous KK modes  $\Psi_m(z)$ , and there is a mass gap between the massless zero mode and the massive continuous KK modes. The existence of the gap is universal in various kinds of de Sitter 3-brane model [13, 49]. It can be shown that there is no any other bound KK mode beside the zero mode for the potential (4.8).

Next, we consider the scalar perturbation. Following the arguments in Refs. [13, 49], one can get the scalar perturbations in the metric (3.10) with the longitudinal gauge:

$$\begin{aligned} ds_5^2 &= e^{2\sigma(z)} [(g_{MN} + \delta g_{MN}) dx^M dx^N] \\ &= e^{2\sigma(z)} [(1 + 2\phi) dz^2 + (1 + 2\psi) q_{\mu\nu} dx^\mu dx^\nu]. \end{aligned} \quad (4.10)$$

The equations of the scalar perturbation in the Schrödinger-like form are read as [49]:

$$\delta\omega = \frac{1}{\omega'} (-3\psi' + 3\sigma'\phi), \quad (4.11a)$$

$$\phi + 2\psi = 0, \quad (4.11b)$$

$$\phi(x, z) = \frac{\omega'}{e^{3\sigma/2}} \Phi(x, z), \quad (4.11c)$$

$$-\Phi''(x, z) + V_s(z)\Phi(x, z) = \square\Phi(x, z), \quad (4.12)$$

where  $\square \equiv q^{\mu\nu}\nabla_\mu\nabla_\nu$ ,  $\delta\omega$  is the perturbation of background scalar  $\omega$ , and  $V_s(z)$  is the effective potential of the scalar perturbation with the expression

$$V_s(z) = -\frac{5}{2}\sigma'' + \frac{9}{4}\sigma'^2 + \sigma'\frac{\omega''}{\omega'} - \frac{\omega'''}{\omega'} + 2\left(\frac{\omega''}{\omega'}\right)^2 - 6\beta^2. \quad (4.13)$$

Now we decompose  $\Phi(x, z)$  according to (4.12) in the form

$$\Phi(x, z) = X(x)f(z). \quad (4.14)$$

Then substitute it into Eq. (4.12), we get

$$\square X(x) = m^2 X(x), \quad (4.15a)$$

$$-f_m''(z) + V_s(z)f_m(z) = m^2 f_m(z). \quad (4.15b)$$

where  $m$  is the 4-dimensional effective mass of the scalar perturbational field. Now Eq. (4.15a) can be explicitly expressed as

$$\begin{aligned} \square X(x) &\equiv q^{\mu\nu} \nabla_\mu \nabla_\nu X(x) = q^{\mu\nu} \left( \partial_\mu \partial_\nu - \Gamma_{\mu\nu}^\lambda \partial_\lambda \right) X(x) \\ &= \left( -\partial_t^2 + e^{-2\beta t} \delta^{ij} \partial_i \partial_j - 3\beta \partial_t \right) X(x) = m^2 X(x), \end{aligned} \quad (4.16)$$

i.e.,

$$e^{2\beta t} \left( \partial_t^2 + 3\beta \partial_t + m^2 \right) X(x) = \delta^{ij} \partial_i \partial_j X(x). \quad (4.17)$$

So  $X(x)$  can be decomposed as

$$X(x) = T_{km}(t) S_k(x^i). \quad (4.18)$$

Then we get

$$\delta^{ij} \partial_i \partial_j S_k(x^i) = -\vec{k}^2 S_k(x^i), \quad (4.19a)$$

$$\ddot{T}_{km}(t) + 3\beta \dot{T}_{km}(t) + \left( e^{-2\beta t} \vec{k}^2 + m^2 \right) T_{km}(t) = 0. \quad (4.19b)$$

The solution of Eq. (4.19a) is simply achieved as  $S_k(x^i) = c e^{-i\delta_{ij} k^i x^j}$ , where  $c$  is a constant. Thus we will focus on Eq. (4.19b). The solution is

$$\begin{aligned} T_{km}(t) &= \frac{1}{2\sqrt{2}} \left( \frac{|\vec{k}|}{\beta} e^{-\beta t} \right)^{\frac{3}{2}} \left[ c_1 \Gamma \left( 1 - \frac{\varsigma}{\beta} \right) \text{J} \left( -\frac{\varsigma}{\beta}, \frac{|\vec{k}|}{\beta} e^{-\beta t} \right) \right. \\ &\quad \left. + c_2 \Gamma \left( 1 + \frac{\varsigma}{\beta} \right) \text{J} \left( \frac{\varsigma}{\beta}, \frac{|\vec{k}|}{\beta} e^{-\beta t} \right) \right], \end{aligned} \quad (4.20)$$

where  $c_1$  and  $c_2$  are integration constants,  $\varsigma = \sqrt{\frac{9}{4}\beta^2 - m^2}$ , and  $\text{J}$  is the Bessel function.

Now we expand  $T_{km}(t)$  about the point  $\frac{|\vec{k}|}{\beta} e^{-\beta t} \sim 0$  ( $t \rightarrow \infty$ ):

$$\begin{aligned} T_{km}(t) &= c_1 2^{-\frac{3}{2} + \frac{\varsigma}{\beta}} \left( \frac{|\vec{k}|}{\beta} e^{-\beta t} \right)^{\frac{3}{2} - \frac{\varsigma}{\beta}} + \mathcal{O} \left( \left( \frac{|\vec{k}|}{\beta} e^{-\beta t} \right)^{\frac{5}{2} - \frac{\varsigma}{\beta}} \right) \\ &\quad + c_2 2^{-\frac{3}{2} - \frac{\varsigma}{\beta}} \left( \frac{|\vec{k}|}{\beta} e^{-\beta t} \right)^{\frac{3}{2} + \frac{\varsigma}{\beta}} + \mathcal{O} \left( \left( \frac{|\vec{k}|}{\beta} e^{-\beta t} \right)^{\frac{5}{2} + \frac{\varsigma}{\beta}} \right) \\ &= c'_1 e^{-(\frac{3}{2}\beta - \varsigma)t} + \mathcal{O} \left( e^{-(\frac{5}{2}\beta - \varsigma)t} \right) + c'_2 e^{-(\frac{3}{2}\beta + \varsigma)t} + \mathcal{O} \left( e^{-(\frac{5}{2}\beta + \varsigma)t} \right), \end{aligned} \quad (4.21)$$

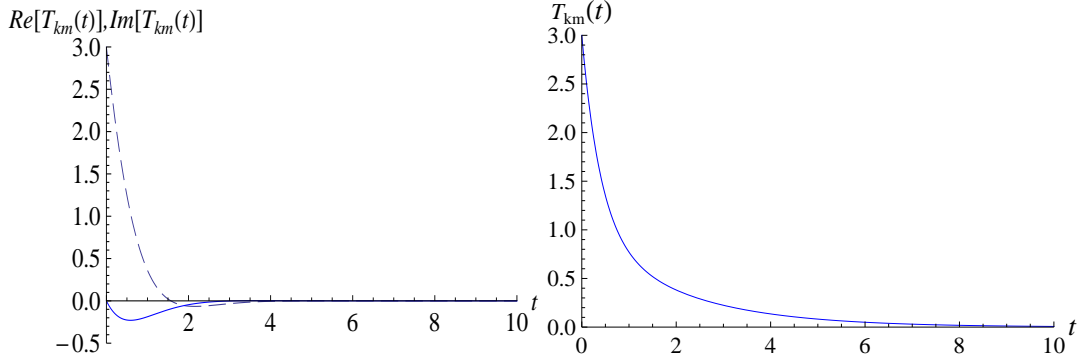
where  $c'_1$  and  $c'_2$  are constants independent of time.

**Case 1:** When  $m^2 > \frac{9}{4}\beta^2$ ,  $\varsigma$  is imaginary. We define  $\varsigma = i\zeta$  with  $\zeta > 0$ . Now (4.21) can be rewritten as

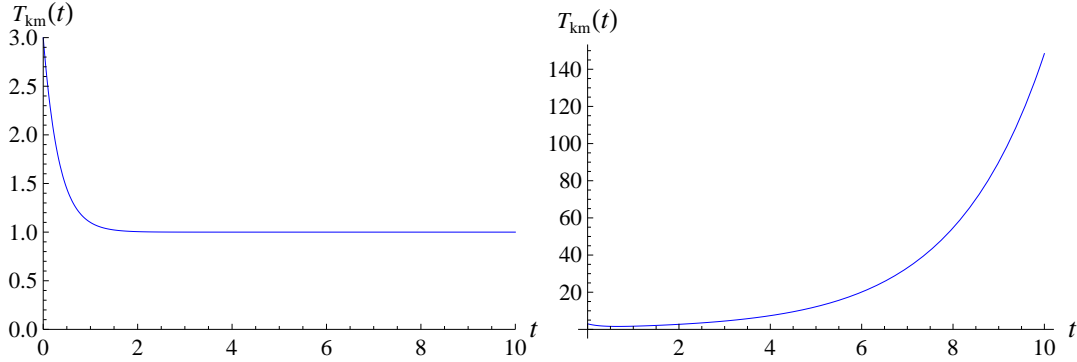
$$T_{km}(t) = c'_1 e^{-(\frac{3}{2}\beta - i\zeta)t} + c'_2 e^{-(\frac{3}{2}\beta + i\zeta)t}. \quad (4.22)$$

Fig. 8a shows that, in this case,  $T_{km}(t)$  vanishes at  $t \rightarrow \infty$ , i.e, the scalar perturbation disappears after a period of time. So we can see the structure is stable in this case.

**Case 2:** When  $0 < m^2 \leq \frac{9}{4}\beta^2$ ,  $\varsigma$  is real and satisfy  $0 \leq \varsigma < \frac{3}{2}\beta$ . Eq. (4.21) shows that  $T_{km}(t)$  is actually suppressed by  $t$ , and vanishes at  $t \rightarrow \infty$ , just as shown in Fig. 8b. So the structure is also stable in this case.



**Figure 8:** The shapes of the function  $T_{km}(t)$  in case 1 (left) and case 2 (right). In case 1, the real part of  $T_{km}(t)$  is denoted by the dash line, and the imaginary part is by the thin line. The parameters are set to  $c'_1 = 1$ ,  $c'_2 = 2$ , and  $\beta = 1$ .



**Figure 9:** The shapes of the function  $T_{km}(t)$  in case 3 (left) and case 4 (right). The parameters are set to  $c'_1 = 1$ ,  $c'_2 = 2$ , and  $\beta = 1$ .

**Case 3:** When  $m^2 = 0$ ,  $\varsigma = \frac{3}{2}\beta$ , the high order terms  $\mathcal{O}(e^{-(\frac{5}{2}\beta - \varsigma)t})$  and  $\mathcal{O}(e^{-(\frac{5}{2}\beta + \varsigma)t})$  in the expanding expression (4.21) are suppressed by  $t$ . While the first term in (4.21) is a constant  $c'_1 = c_1$ . If  $c_1 = 0$ ,  $T_{km}(t)$  also converges to zero when  $t \rightarrow \pm\infty$ , so the structure is stable. If  $c_1 \neq 0$ ,  $T_{km}(t)$  will converge to the constant  $c_1$  (see Fig. 9a), i.e., some slight scalar perturbations will always exist but not enormously affect the stability of the brane. So in this case we can say that the structure is also stable.

**Case 4:** When  $m^2 < 0$ ,  $\varsigma$  is real and satisfy  $\varsigma > \frac{3}{2}\beta$ , the first term in (4.21) is divergent at  $t \rightarrow \infty$  (see Fig. 9b). This means that in this case the scalar perturbation is divergent, and the structure is unstable under the scalar perturbation.

From above discussion, it is shown that the structure is stable when  $m^2 \geq 0$ , while it is unstable when  $m^2 < 0$ .

We next focus on Eq. (4.15b), where  $V_s(z)$  is the effective potential of the scalar perturbation. For (3.16a) and (3.16b), we have

$$\begin{aligned} V_s(z) &= -\frac{5}{2}\sigma'' + \frac{9}{4}\sigma'^2 + \sigma' \frac{\omega''}{\omega'} - \frac{\omega'''}{\omega'} + 2 \left( \frac{\omega''}{\omega'} \right)^2 - 6\beta^2 \\ &= \frac{3}{4}\beta^2 [3 + \text{sech}^2(2\beta z)]. \end{aligned} \quad (4.23)$$

From the expression of the above effective scalar perturbational potential, we can see that

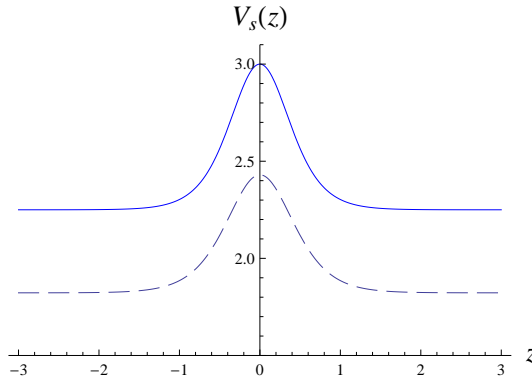


**Figure 10:** The shapes of the potential  $V_s(z)$ . The parameter  $\beta$  is set to  $\beta = 0.9$  for the dashed line, and  $\beta = 1$  for the thin line.

$V_s(z)$  approaches to  $\frac{9}{4}\beta^2$  when  $z \rightarrow \pm\infty$ . Furthermore,  $V_s(z)$  satisfies  $V_s(z) > \frac{9}{4}\beta^2$  and is always convex and non-negative. Fig. 10 shows the potential with various cases about the parameter  $\beta$ . From the Schrödinger-like equation (4.15b), we can conclude that there are only KK modes with eigenvalues  $m^2 > \frac{9}{4}\beta^2$ . This coincides with case 1. So the structure is stable under the scalar perturbations. The explicit argument about the stable problem of scalar perturbations could be seen in Ref. [49].

The coordinate system corresponding to the four-dimensional metric  $q_{\mu\nu}$  in (3.4) is not a global one. However, even if we use a global coordinate system, we will find the same results as the previous discussion, namely, the scalar perturbation will ultimately vanish, approach a constant, and diverge for the cases of  $m^2 > 0$ ,  $m^2 = 0$ , and  $m^2 < 0$ , respectively. So this consequence results from the property of the four-dimensional background space-time. On the other hand, Eq. (4.15a) is just a Klein-Gordon equation. If the background is a flat Minkowski space-time, the solution is just a plane wave which never vanishes and diverges. But now the background is a de Sitter space-time. There is an exponential expansion factor  $e^{2\beta t}$  before the space components, that means the space will exponentially expand with time. As a consequence, the symmetries of a de Sitter space-time are very

different from that of a Minkowski one. However, the space is still homogeneous and isotropic in de Sitter case, so the solution respect to the Eq. (4.19a) has the same form as in a Minkowski space-time, i.e.,  $S_k(x^i) = ce^{-i\delta_{ij}k^i x^j}$ . But the solution of time component will change and we find that the amplitude will ultimately vanish especially for  $m^2 > 0$  in de Sitter case. Then from Eqs. (4.22) and (4.14), we can see that  $\Phi(x, z)$  will approach to zero. Therefore, from (4.11), we know that the scalar perturbations  $\phi$ ,  $\psi$  and  $\delta\omega$  will ultimately vanish.

In what follows, we will address the question of how the perturbations couple to matter fields on the brane. However, since the scalar perturbations  $\phi$ ,  $\psi$  and  $\delta\omega$  ultimately vanish, their interaction with matter fields will decouple finally. So we only consider the interaction of the tensor perturbations couple to matter fields on the brane, which will lead to the effective Newtonian potential on the brane.

## 5. The Effective Newtonian Potential

In Section 4, we have considered the gravitational perturbation and achieved a Schrödinger equation (4.7). In order to have localized four-dimensional gravity, we should require that the KK modes of the Schrödinger equation (4.7) don't lead to unacceptably large corrections to the Newtonian potential in four-dimensional theory. In the thick brane scenario the matter fields in the four-dimensional theory on the brane would be smeared over the fifth dimension. For simplicity, like in Refs. [1, 2, 50, 51, 52], we consider the gravitational potential between two point-like sources of mass  $M_1$  and  $M_2$  located at the origin of the fifth-dimension, i.e.,  $z = 0$ . This assumption is justified in case when the thickness of the brane is small compared with the bulk curvature. The effective potential between these two particles is given by the exchange of the massless zero mode and KK massive modes. And the zero mode will cause a four-dimensional Newtonian interaction potential, the continuum KK modes will produce the correction to the potential. Thus the effective potential is given by [51]:

$$U(r) = G_N \frac{M_1 M_2}{r} + \frac{M_1 M_2}{M_*^3} \int_{m_0}^{\infty} dm \frac{e^{-mr}}{r} |\Psi_m(0)|^2, \quad (5.1)$$

where  $G_N = M_4^{-2}/16\pi$  is the four-dimensional coupling constant, i.e., the Newton's gravitational constant,  $M_* = (16\pi G_5)^{-1/3}$  is the fundamental five-dimensional Planck scale, and  $m_0$  is the minimal eigenvalue at which the continuum KK modes start. In our model,  $m_0$  is not zero but  $3\beta/2$  because there is a gap in the mass spectrum.

As in [5], consider the four-dimensional perturbational metric factors in (3.10)

$$d\hat{s}_5^2 = e^{2\sigma(z)} [(q_{\mu\nu} + h_{\mu\nu}(x)) dx^\mu dx^\nu + dz^2], \quad (5.2)$$

We decompose the five-dimensional action (2.3) into a four dimensional and higher dimensional parts, i.e.,

$$S_5^R \supset M_*^3 \int d^5x \sqrt{\hat{g}} \hat{R} \supset M_*^3 \int_{-\infty}^{\infty} dz e^{3\sigma(z)} \int d^4x \sqrt{\hat{g}^{(4)}} \hat{R}^{(4)} = M_4^2 \int d^4x \sqrt{\hat{g}^{(4)}} \hat{R}^{(4)}, \quad (5.3)$$



where  $\hat{R}^{(4)}$  is the four-dimensional Ricci scalar made out of  $\hat{g}_{\mu\nu}^{(4)} = q_{\mu\nu} + h_{\mu\nu}(x)$ . So we can read off the relation of the effective four-dimensional Planck scale  $M_4$  and the fundamental five-dimensional Planck scale  $M_*$ ,

$$M_4^2 = M_*^3 \int_{-\infty}^{\infty} dz e^{3\sigma(z)} = \sqrt{\frac{2}{\pi}} \Gamma^2\left(\frac{3}{4}\right) \frac{M_*^3}{\beta} \approx 1.2 \frac{M_*^3}{\beta}. \quad (5.4)$$

We note that since  $M_4 = M_{pl}$  and the fundamental five-dimensional Planck scale  $M_*$  is not fixed, the order of  $M_*$  is decided by the de Sitter parameter  $\beta$ . However, an analogue relation can be found in RS2 model [1, 6],  $M_4^2 = M_*^3/k$ , where  $k$  appearing in the warp factor of RS metric is a scale of order the Planck scale and  $k^{-1}$  represents the anti-de Sitter radius. Thus  $M_* \sim M_{pl}$  in RS2 model. From Eq. (5.4), if we chose  $\beta \sim M_{pl}$ ,  $M_*$  is of order the Planck scale in our model.

In order to get the continuum modes, substituting (4.8) into (4.7) and introducing a new variable  $l = 2\beta z$ , we can reform the Schrödinger equation as a simple form:

$$-\Psi''(l) - \frac{21}{16} \text{sech}^2(l) \Psi(l) = M^2 \Psi(l), \quad (5.5)$$

where the prime denotes derivative with respect to the coordinate  $l$ , and the new eigenvalue is  $M = \sqrt{\frac{m^2}{4\beta^2} - \frac{9}{16}}$ . Since in our model, the continuum KK modes start at  $m \geq 3\beta/2$ , so when we just consider these continuum modes,  $M$  will be a nonnegative real number. The solution of this equation is given by a linear combination of the associated Legendre functions:

$$\Psi_M(l) = C_1 P\left(\frac{3}{4}, iM, \tanh(l)\right) + C_2 Q\left(\frac{3}{4}, iM, \tanh(l)\right), \quad (5.6)$$

where  $C_1, C_2$  are  $M$ -dependent parameters. When  $l \rightarrow \infty$ , each KK mode wave function will approach to a plane wave:

$$\Psi_M(l) = K_1 e^{iMl} + K_2 e^{-iMl} \quad (5.7)$$

with the parameters  $K_1$  and  $K_2$  given by

$$K_1 = \frac{2C_1 - i\pi C_2 \coth(\pi M)}{2\Gamma(1 - iM)},$$

$$K_2 = \frac{C_2}{2C_M [2 \sinh^2(M\pi) + i \sinh(2\pi M)]},$$

where  $C_M = \frac{4^{iM}}{8\pi^{3/2}} (3 + 8iM + 16M^2) \Gamma(1 + iM) \Gamma(-\frac{3}{2} - 2iM)$ . Further, we chose the parameters  $K_1 = K_2 = 1/2$  to normalize the plane wave function  $\Psi_M(l)$ , so the parameters  $C_1$  and  $C_2$  are fixed as:

$$C_1 = \frac{\pi}{2} C_M [2 \cosh^2(\pi M) - i \sinh(2\pi M)] + \frac{1}{2} \Gamma(1 - iM),$$

$$C_2 = -C_M [2 \sinh^2(M\pi) + i \sinh(2\pi M)].$$

Substitute  $C_1$  and  $C_2$  into Eq. (5.6), we will achieve the whole wave functions of the continuum KK modes  $\Psi_M(l)$ . Now replace  $l$  with  $2\beta z$  and  $M$  with  $\sqrt{\frac{m^2}{4\beta^2} - \frac{9}{16}}$  in the

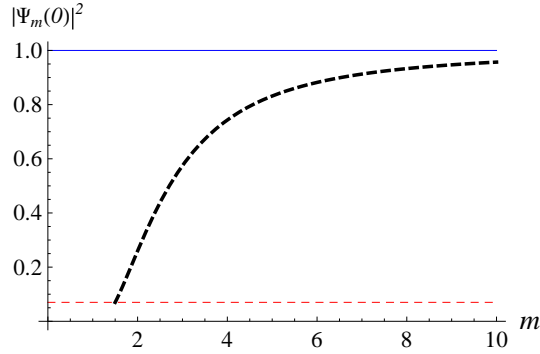


**Figure 11:** The shape of  $|\Psi_m(0)|^2$  as a function of  $m$ . The black dashed line represents  $|\Psi_m(0)|^2$ , the red dashed line represents the constant 0.070, and the blue thin line represents the constant 1. The parameter is set to  $\beta = 1$ .

function  $\Psi_M(l)$ , we transform  $\Psi_M(l)$  back into  $\Psi_m(z)$  which refers to the KK modes wave function in original Schrödinger equation (4.7). We display the curve of  $|\Psi_m(0)|^2$  as a function of  $m$  in Fig. 11. It is shown that  $|\Psi_m(0)|^2$  will approach to 1 with the increase of the mass  $m$ . The reason is that the wave function  $\Psi_m(z)$  approximates to a normalized plane wave as the eigenvalue  $m$  become large. On the other hand, the value of  $|\Psi_{m_0}|^2$  is a constant  $\pi/[\Gamma(1/8)\Gamma(11/8)]^2 = 0.070$  and independent of the parameter  $\beta$ .

Now we focus on the Newtonian potential correction term in Eq. (5.1). We write the integrand as:

$$I(m) = \frac{e^{-mr}}{r} |\Psi_m(0)|^2. \quad (5.8)$$

Because it can not be analytically integrated, we will deal with the complex integrand  $I(m)$  under some simple cases for which the integral can easily achieved.

**Case 1:** We replace all the KK mode wave functions  $\Psi_m(0)$  with the lowest mode  $\Psi_{m_0}(0)$ . In this case,  $|\Psi_m(0)|^2$  will be replaced by  $\pi/[\Gamma(1/8)\Gamma(11/8)]^2 = 0.070$ . Now the integrand is simply given by

$$I_1(m) = 0.070 \frac{e^{-mr}}{r}. \quad (5.9)$$

So in this case the correction of the Newtonian potential is

$$\Delta U_1(r) = 0.070 \frac{e^{-3r\beta/2}}{M_*^3} \frac{M_1 M_2}{r^2}. \quad (5.10)$$

**Case 2:** We replace  $|\Psi_m(0)|^2$  with the constant 1, which refers to the limit  $|\Psi_\infty(0)|^2$  when  $m \rightarrow \infty$ . In this case, all KK modes are approximately considered as the plane waves. So we have

$$I_2(m) = \frac{e^{-mr}}{r}. \quad (5.11)$$

The correction of the Newtonian potential is given by

$$\Delta U_2(r) = \frac{e^{-3r\beta/2}}{M_*^3} \frac{M_1 M_2}{r^2}. \quad (5.12)$$

**Case 3:** The wave function  $|\Psi_m(0)|^2$  approaches to a constant 1 when  $m$  is large and the exponent  $e^{-mr}$  is strongly suppressed by large  $m$ , so the integrand is mostly determined by the contribution of smaller mass modes. For this point, we can expand  $|\Psi_m(0)|^2$  about the point  $m_0 = 3\beta/2$ :

$$|\Psi_m(0)|^2 = 0.037 - 0.079\frac{m^2}{\beta^2} + 0.042\frac{m^4}{\beta^4} + \mathcal{O}\left(\frac{m^6}{\beta^6}\right). \quad (5.13)$$

So the integrand now can be expressed as

$$I_3(m) = \left(0.037 - 0.079\frac{m^2}{\beta^2} + 0.042\frac{m^4}{\beta^4}\right) \frac{e^{-mr}}{r}. \quad (5.14)$$

In this case, the correction can be write as

$$\Delta U_3(r) = \frac{e^{-3r\beta/2}M_1M_2}{M_*^3} \left(\frac{0.072}{r^2} + \frac{0.330}{\beta r^3} + \frac{0.976}{r^4\beta^2} + \frac{1.512}{r^5\beta^3} + \frac{1.008}{r^6\beta^4}\right). \quad (5.15)$$

In order to distinguish which case above is more accurate compared to the original correction of Newtonian potential, we can compare the precise integrand (5.8) with the above three approximate cases (5.9), (5.11) and (5.14) at some fixed distances  $r$  of the two particles. Since the area under an integrand curve represents the integrate value of it, so by comparing the areas of three cases with the precise condition, we can fixed a suitable form of the correction. Now we display the curves of the precise and above three approximate cases with some different fixed distances in Fig. 12 and 13.

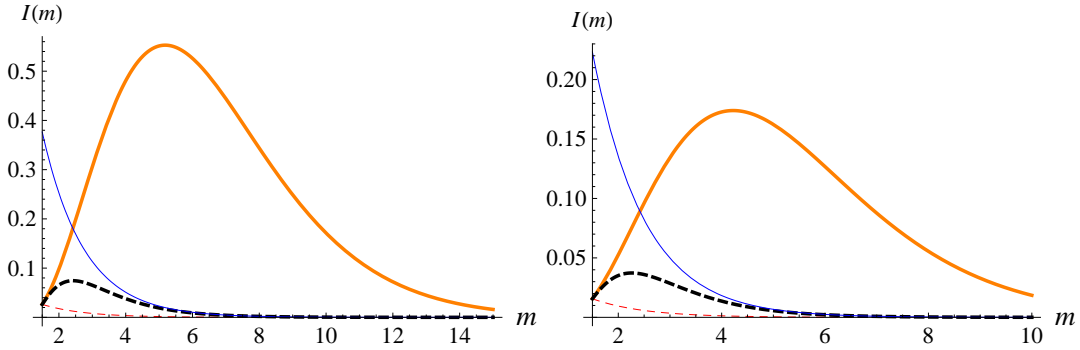


**Figure 12:** The integrand curves of the precise and three approximate cases with fixed distances  $r = 0.8$  (left) and  $r = 1$  (right). The black dashed thick lines represent the precise integrand curve, the red dashed thin lines represent case 1, the blue thin lines represent case 2, and the orange thick lines represent case 3. The parameter is set to  $\beta = 1$ .

We find that the integrand (5.14) in case 3 largely deviates from the precise case when  $r$  is small (Fig. 12) but well matches with the precise case when the distance  $r$  is large enough (Fig. 13). The reason is that we replace the function  $|\Psi_m(0)|^2$  in the integrand (5.8) with a polynomial of  $m$ . The polynomial is a good approximation at small  $m$ , and even at large  $m$ , as long as the distance  $r$  is also large. Large  $r$  will lead to the exponent

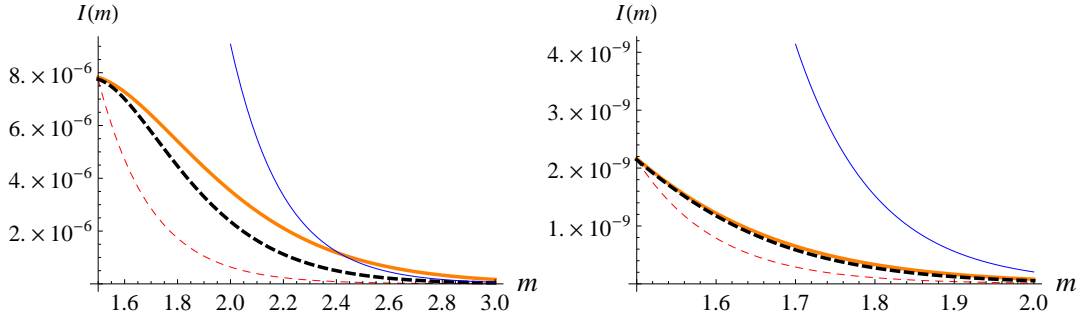


**Figure 13:** The integrand curves of the precise and three approximate cases with fixed distances  $r = 5$  (left) and  $r = 10$  (right). The black dashed thick lines represent the precise integrand curve, the red dashed thin lines represent case 1, the blue thin lines represent case 2, and the orange thick lines represent case 3. The parameter is set to  $\beta = 1$ .

$e^{-mr}$  greatly suppressed, so the polynomial is still a good approximation. However, when  $r$  is small enough,  $e^{-mr}$  will not be very little, but the contribution of the polynomial with large  $m$  will be great, in consequence there will be a obvious derivation with the precise case. This is also can be seen in Eq. (5.15), when  $r$  is small enough, the main terms that will contribute to the correction are the high order terms of  $1/r^2$ , but when  $r$  is large the main term will be  $1/r^2$ . So for this consideration we will not use the correction of case 3 as the approximation of the final correction. On the other hand, we can read from the two figures that the precise integrand curve is always between the curves of case 1 and case 2, and this is obviously, since the Fig. 11 shows that  $0.070 \leq |\Psi_m(0)|^2 \leq 1$ , so these integrands have the relation  $I_1(m) \leq I(m) \leq I_2(m)$ . Hence, the precise correction of Newtonian potential  $\Delta U(r)$  must satisfy  $\Delta U_1(r) < \Delta U(r) < \Delta U_2(r)$ , i.e.,

$$0.070 \frac{e^{-3r\beta/2}}{M_*^3} \frac{M_1 M_2}{r^2} < \Delta U(r) < \frac{e^{-3r\beta/2}}{M_*^3} \frac{M_1 M_2}{r^2}. \quad (5.16)$$

Though the above discussion, we obtain the suitable correction of Newtonian potential:

$$\Delta U(r) = \kappa \frac{e^{-3r\beta/2}}{M_*^3} \frac{M_1 M_2}{r^2}, \quad (5.17)$$

where the parameter  $\kappa$  is a constant satisfied  $0.070 < \kappa < 1$ .

So in our mode the effective Newtonian potential can be written as

$$U(r) = G_N \frac{M_1 M_2}{r} + \kappa \frac{e^{-3r\beta/2}}{M_*^3} \frac{M_1 M_2}{r^2}. \quad (5.18)$$

This is greatly different from the correction caused by a volcano-like effective potential [51, 52]. We can find when the distance  $r$  of the two particles is large, the  $1/r^2$  term is a high order term compared with  $1/r$ , and the exponent  $e^{-3r\beta/2}$  is also greatly suppressed. So in this situation, the correction is tininess and can be negligible. However, when  $r$  is small,  $e^{-3r\beta/2}/r^2$  will be large and could be the main term of the potential.

## 6. Conclusion

In this paper, we consider the de Sitter thick brane solution in Weyl geometry. By performing the conformal transformation to map the Weyl structure into the familiar Riemann one, and further, via a coordinate transformation  $dy = e^{A(z)}dz$  to transform the metric into a conformal one, we transform the structure to a de Sitter thick brane on Riemann manifold. The solution is

$$U(\omega) = 5\beta^2 \left[ \cos^2 \left( \frac{\omega}{\sqrt{3}} \right) - \frac{1}{2} \right] e^{-\omega}, \quad (6.1)$$

$$\omega(z) = \frac{\sqrt{3}}{2} \arctan [\sinh(2\beta z)], \quad (6.2)$$

$$e^{2A(z)} = e^{\sqrt{3} \arctan[\sinh(2\beta z)]} \operatorname{sech}(2\beta z). \quad (6.3)$$

The scalar field  $\omega$  is a kink solution and preserves symmetry with respect to  $z$  coordinate, while the scalar potential  $U(\omega)$  and warp factor  $e^{2A}$  are asymmetric. But actually,  $z$  coordinate is not a real physical one. After transforming back to the physical  $y$  coordinate with  $dy = e^{A(z)}dz$ , we find that all magnitudes are not preserving symmetry with extra coordinate  $y$ . The energy density is still localized around the origin of coordinate, while our matter distribution on the de Sitter brane is asymmetric along the extra dimension.

Then we consider the perturbations in the metric (3.10) in Riemann structure. For gravitational perturbation, we get a Pöschl-Teller-like potential for the gravitational KK modes. It is found that there is a normalizable massless gravitational zero mode localized on the brane, and exists a mass gap between the zero mode and the massive continuous KK modes. The existence of such a mass gap also conforms to the universal phenomenon in various de Sitter 3-brane models. And for scalar perturbation, it is shown that the scalar perturbations will ultimately vanish, so the solution is stable in this perturbation.

Finally, we discuss the effective Newtonian potential on the brane, and find the correction term is proportional to  $e^{-3r\beta/2}/r^2$ , which is greatly different from the correction caused by a volcano-like effective potential. This result shows that the perturbations don't lead to unacceptably large corrections to the Newtonian potential in four-dimensional theory.

## 7. Acknowledgments

We are grateful to the referee, whose comments led to the improvement of this paper. This work was supported by the Program for New Century Excellent Talents in University, the National Natural Science Foundation of China (No. 10705013), the Doctoral Program Foundation of Institutions of Higher Education of China (No. 20070730055 and No. 20090211110028), the Key Project of Chinese Ministry of Education (No. 109153), the Natural Science Foundation of Gansu Province, China (No. 096RJZA055), and the Fundamental Research Funds for the Central Universities (No. lzujbky-2009-54).

## References

- [1] V.A. Rubakov, *Large and infinite extra dimensions*, Phys. Usp. **44** (2001) 871, arXiv:hep-ph/0104152.
- [2] C. Csáki, *TASI Lectures on Extra Dimensions and Branes*, arXiv:hep-ph/0404096.
- [3] N. Arkani-Hamed, S. Dimopoulos and G. Dvali, *The hierarchy problem and new dimensions at a millimeter*, Phys. Lett. **B 429** (1998) 263;
- [4] I. Antoniadis, N. Arkani-Hamed, S. Dimopoulos and G. Dvali, *New dimensions at a millimeter to a Fermi and superstrings at a TeV*, Phys. Lett. **B 436** (1998) 257.
- [5] L. Randall and R. Sundrum, *A Large Mass Hierarchy from a Small Extra Dimension*, Phys. Rev. Lett. **83** (1999) 3370;
- [6] L. Randall and R. Sundrum, *An alternative to compactification*, Phys. Rev. Lett. **83** (1999) 4690.
- [7] C. Csáki, M. Graesser, C. Kolda and J. Terning, *Cosmology of One Extra Dimension with Localized Gravity*, Phys. Lett. **B 462** (1999) 34, arXiv:hep-ph/9906513;
- [8] J.M. Cline, C. Grojean and G. Servant, *Cosmological Expansion in the Presence of an Extra Dimension*, Phys. Rev. Lett. **83** (1999) 4245, arXiv:hep-ph/9906523.
- [9] O. DeWolfe, D.Z. Freedman, S.S. Gubser and A. Karch, *Modeling the fifth dimension with scalars and gravity*, Phys. Rev. **D 62** (2000) 046008.
- [10] M. Gremm, *Four-dimensional gravity on a thick domain wall*, Phys. Lett. **B 478** (2000) 434.
- [11] C. Csáki, J. Erlich, T. Hollowood and Y. Shirman, *Universal Aspects of gravity localized on thick branes*, Nucl. Phys. **B 581** (2000) 309.
- [12] A. Campos, *Critical phenomena of thick brane in warped space-time*, Phys. Rev. Lett. **88** (2002) 141602.
- [13] A.Z. Wang, *Thick de Sitter brane worlds, dynamic black holes and localization of gravity*, Phys. Rev. **D 66** (2002) 024024, arXiv:hep-th/0201051.
- [14] O. Arias, R. Cardenas and I. Quiros, *Thick Brane Worlds Arising From Pure Geometry*, Nucl. Phys. **B 643** (2002) 187, arXiv:hep-th/0202130.
- [15] V. Dzhunushaliev, V. Folomeev and M. Minamitsuji, *Thick de Sitter brane solutions in higher dimensions*, Phys. Rev. **D 79** (2009) 024001, arXiv:0809.4076[gr-qc].
- [16] V. Dzhunushaliev, V. Folomeev and M. Minamitsuji, *Thick brane solutions*, Rept. Prog. Phys. **73** (2010) 066901, arXiv:0904.1775[gr-qc].
- [17] A. Herrera-Aguilar, D. Malagn-Morejn, R.R. Mora-Luna, U. Nucamendi, *Aspects of thick brane worlds: 4D gravity localization, smoothness, and mass gap*, Mod. Phys. Lett. **A 25** (2010) 2089, arXiv:0910.0363[hep-th].
- [18] C.A.S. Almeida, M.M. Ferreira Jr., A.R. Gomes, R. Casana, *Fermion localization and resonances on two-field thick branes*, Phys. Rev. **D 79** (2009) 125022, arXiv:0901.3543[hep-th].
- [19] Y.-X. Liu, L. Zhao and Y.-S. Duan, *Localization of Fermions on a String-like Defect*, JHEP **0704** (2007) 097;

- [20] L. Zhao, Y.-X. Liu and Y.-S. Duan, *Fermions in gravity and gauge backgrounds on a brane world*, Mod. Phys. Lett. **A 23** (2008) 1129.
- [21] Y.-X. Liu, J. Yang, Z.-H. Zhao, C.-E Fu, Y.-S. Duan, *Fermion Localization and Resonances on A de Sitter Thick Brane*, Phys. Rev. **D 80** (2009) 065019, arXiv:0904.1785[hep-th];
- [22] Y.-X. Liu, C.-E Fu, L. Zhao, Y.-S. Duan, *Localization and Mass Spectra of Fermions on Symmetric and Asymmetric Thick Branes*, Phys. Rev. **D 80** (2009) 065020, arXiv:0907.0910[hep-th];
- [23] Y.-X. Liu, H.-T. Li, Z.-H. Zhao, J.-X. Li, J.-R. Ren, *Fermion Resonances on Multi-field Thick Branes*, JHEP **10** (2009) 091, arXiv:0909.2312[hep-th].
- [24] W.T. Cruz, M.O. Tahim and C.A.S. Almeida, *Scalar and tensor gauge field localization on deformed thick branes*, arXiv:0906.1850[hep-th].
- [25] L.-J. Zhang and G.-H. Yang, *Zero Modes of Matter Fields on Scalar Flat Thick Branes*, arXiv:0907.1178[hep-th].
- [26] D. Bazeia, F.A. Brito and J.R. Nascimento, *Supergravity brane worlds and tachyon potentials*, Phys. Rev. **D 68** (2003) 085007;
- [27] D. Bazeia and A.R. Gomes, *Bloch Brane*, JHEP **0405** (2004) 012;
- [28] D. Bazeia, F.A. Brito and L. Losano, *Scalar fields, bent branes, and RG flow*, JHEP **0611** (2006) 064;
- [29] D. Bazeia, A.R. Gomes, L. Losano and R. Menezes, *Braneworld Models of Scalar Fields with Generalized Dynamics*, Phys. Lett. **B 671** (2009) 402.
- [30] K. Farakos, N.E. Mavromatos and P. Pasipoularides, *Asymmetrically Warped Brane Models, Bulk Photons and Lorentz Invariance*, J. Phys. Conf. Ser. **189** (2009) 012029, arXiv:0902.1243[hep-th];
- [31] E. O’Callaghan, R. Gregory and A. Poursidou, *The Cosmology of Asymmetric Brane Modified Gravity*, JCAP **0909** (2009) 020, arXiv:0904.4182[astro-ph.CO];
- [32] P. Koroteev and M. Libanov, *Spectra of Field Fluctuations in Braneworld Models with Broken Bulk Lorentz Invariance*, Phys. Rev. **D 79** (2009) 045023, arXiv:0901.4347[hep-th];
- [33] A. Flachi, M. Minamitsuji, *Field localization on a brane intersection in anti-de Sitter spacetime*, Phys. Rev. **D 79** (2009) 104021, arXiv:0903.0133[hep-th].
- [34] D. Puetzfeld, *Status of non-Riemannian cosmology*, New Astron. Rev. **49** (2005) 59.
- [35] N. Barbosa-Cendejas and A. Herrera-Aguilar, *Localization of 4D gravity on pure geometrical thick branes*, Phys. Rev. **D 73** (2006) 084022; Erratum-ibid. **D 77** (2008) 049901, arXiv:hep-th/0603184.
- [36] N. Barbosa-Cendejas and A. Herrera-Aguilar, *4D gravity localized in non  $Z_2$ -symmetric thick branes*, JHEP **0510** (2005) 101.
- [37] N. Barbosa-Cendejas, A. Herrera-Aguilar, M. A. Reyes and C. Schubert, *Mass gap for gravity localized on Weyl thick branes*, Phys. Rev. **D 77** (2008) 126013.
- [38] Y.-X. Liu, L.-D. Zhang, S.-W. Wei and Y.-S. Duan, *Localization and Mass Spectrum of Matters on Weyl Thick Branes*, JHEP **0808** (2008) 041, arXiv:0803.0098[hep-th].

- [39] Y.-X. Liu, X.-H. Zhang, L.-D. Zhang and Y.-S. Duan, *Localization of Matters on Pure Geometrical Thick Branes*, JHEP **0802** (2008) 067, arXiv:0708.0065[hep-th].
- [40] M. Minamitsuji, W. Naylor and M. Sasaki, *Quantum fluctuations on a thick de Sitter brane*, Nucl. Phys. **B 737** (2006) 121.
- [41] M. Minamitsuji, W. Naylor and M. Sasaki, *Can thick braneworlds be self-consistent?* Phys. Lett. **B 633** (2006) 607, arXiv:hep-th/0510117.
- [42] R. Guerrero, R. Ortiz, R.O. Rodriguez and R.S. Torrealba, *De Sitter and double irregular domain walls*, Gen. Rel. Grav. **38** (2006) 845, arXiv:gr-qc/0504080.
- [43] R. Guerrero, R.O. Rodriguez and R.S. Torrealba, *De-Sitter and double asymmetric brane worlds*, Phys. Rev. **D 72** (2005) 124012, arXiv:hep-th/0510023.
- [44] R. Goetz, *The gravitational field of plane symmetric thick domain walls*, J. Math. Phys. **31** (1990) 2683.
- [45] R. Gass and M. Mukherjee, *Domain wall spacetimes and particle motion*, Phys. Rev. **D 60** (1999) 065011.
- [46] Y.-X. Liu, Z.-H. Zhao, S.-W. Wei and Y.-S. Duan, *Bulk Matters on Symmetric and Asymmetric de Sitter Thick Branes*, JCAP **02** (2009) 003, arXiv:0901.0782[hep-th].
- [47] R. Koley, S. Kar, *Scalar kinks and fermion localisation in warped spacetimes*, Class. Quant. Grav. **22** (2005) 753, arXiv:hep-th/0407158.
- [48] Y.-X. Liu, L.-D. Zhang, L.-J. Zhang and Y.-S. Duan, *ermions on Thick Branes in Background of Sine-Gordon Kinks* Phys. Rev. **D 78** (2008) 065025, arXiv:0804.4553[hep-th].
- [49] S. Kobayashi, K. Koyama and J. Soda, *Thick Brane Worlds and Their Stability*, Phys. Rev. **D 65** (2002) 064014, arXiv:hep-th/0107025.
- [50] N. Arkani-Hamed, S. Dimopoulos, G. Dvali, N. Kaloper, *Infinitely Large New Dimensions*, Phys. Rev. Lett. **84** (2000) 586, arXiv:hep-th/9907209.
- [51] C. Csaki, J. Erlich, T.J. Hollowood and Y. Shirman, *Universal Aspects of Gravity Localized on Thick Branes*, Nucl. Phys. **B 581** (2000) 309, arXiv:hep-th/0001033.
- [52] D. Bazeia, A.R. Gomes and L. Losano, *Gravity localization on thick branes: a numerical approach*, Int. J. Mod. Phys. **A 24** (2009) 1135, arXiv:hep-th/0708.3530.